Bulletin of Geophysics and Oceanography Vol. XX, n. X, pp. XXX-XXX; Xxxxx 20xx
DOI 10.4430/bgo00548

Assessment of seismic susceptibility in a seismotectonically active coastal zone using GIS-AHP: the case of Bandırma, Turkey

A. Saraçoğlu

Department of Civil Engineering, Technology Faculty, Firat University, Elazig, Turkey

(Received: 30 March 2026; accepted: 15 September 2026; published online: 12 November 2026)

ABSTRACT Rapid urbanisation in seismotectonically active regions requires robust spatial methodologies for assessing seismic susceptibility. This study presents a geo-environmental multi-criteria approach to evaluate the regional seismic susceptibility of Bandırma, Turkey, a coastal city under the continuous threat of the North Anatolian Fault. An integrated geographic information system and analytical hierarchy process (AHP) framework was developed using four primary criteria: distance to seismogenic fault lines, lithology, groundwater level, and slope. To address complex hydrogeological conditions, a nested AHP sub-model derived shallow groundwater accumulations from eight environmental factors, explicitly accounting for seismically-induced liquefaction potential in saturated soils. The resulting zonation classified the region into five susceptibility categories, revealing that 16.96% of the area is exposed to high, or very high, seismic susceptibility, predominantly in zones underlain by unconsolidated Quaternary alluvium within near-field fault zones. A sensitivity analysis examined the stability of the zonation under the tested variations in the criteria weights. This study provides a regional seismic susceptibility map that can support preliminary territorial planning, coastal management and risk-informed land-use screening, and help identify areas in which more detailed geotechnical and seismological investigations should be prioritised.

Key words: seismic susceptibility assessment, GIS-AHP, spatial modelling, North Anatolian Fault, land use planning.

1. Introduction

The convergence of accelerated urbanisation and population growth, notably within developing nations, has precipitated an augmented demand for new residential areas over the past century. Seminal works on site selection established foundational models for urban and industrial land use. However, it should be noted that these models were primarily driven by economic and logistical criteria (Herbert and Stevens, 1960; Alonso, 1964; Putman, 1979; Harris, 1985; Amano *et al*., 1987). A critical dimension that has frequently been overlooked in these early frameworks pertains to the vulnerability to natural hazards. This oversight has historically resulted in catastrophic consequences. The selection of settlement locations in tectonically active zones, that is considered improper, continues to be a primary cause of the immense loss of life and economic devastation caused by seismic events. This has been tragically exemplified by the Tangshan (1976), Marmara (1999), and Kahramanmaras (2023) earthquakes.

This context highlights a fundamental challenge in contemporary urban planning: the

© 2026 - The Author(s)

balancing of development imperatives with disaster resilience principles. Contemporary approaches increasingly acknowledge that sustainable urbanism cannot be disentangled from risk-sensitive land-use planning. The notion of disaster resilience encompasses more than mere structural protection; it signifies the capacity of urban systems and communities to prepare for, withstand, and recover from hazardous events. It is imperative to recognise that incorporating hazard assessments into the earliest phases of urban development is not merely a technical undertaking; rather, it is a strategic imperative that underscores the paramount importance of safeguarding lives and ensuring the long-term sustainability of urban areas (Liu *et al*., 2024).

Turkey, being situated within the seismically active Alpine-Himalayan belt, is particularly susceptible to such events. The magnitude of seismic susceptibility is compounded by local geological and geotechnical conditions. In this context, soil characteristics and structural integrity are pivotal in determining the extent of damage (Karaoğlu, 2014). The presence of unfavourable site conditions, such as loose granular soils with a high susceptibility to subsidence or saturated sand deposits that are vulnerable to liquefaction, has been demonstrated to have the capacity to significantly amplify seismic ground motion and to exacerbate structural failure (Robertson and Wride, 1998; Orellana *et al*., 2021). The seismic events that occurred in Marmara (1999), Van (2011), and Kahramanmaras (2023) have highlighted the increased vulnerability of structures constructed on unconsolidated soils in comparison to those erected on solid bedrock (Montoya and Masser, 2005; Değerliyurt, 2014; Jara *et al*., 2022). Consequently, a thorough evaluation of soil characteristics, encompassing the deformation behaviour of the soil (Santamarina *et al*., 2001; Mitchell *et al*., 2005), its bearing capacity (Fredlund, 2006), and the impact of groundwater levels, has emerged as a pivotal component of contemporary disaster-resilient urban planning and site suitability analysis (Collins *et al*., 2001; Malczewski, 2004; Arnous, 2013; Bastani *et al*., 2024; Hajilo *et al*., 2024).

The coastal city of Bandırma, located in north-western Turkey, serves as a critical case study for this research. The city's strategic location in close proximity to active branches of the North Anatolian Fault, one of the world's most active continental transform faults, places it under significant and persistent earthquake threat. Addressing this vulnerability necessitates a multifaceted approach that can systematically evaluate and integrate various risk-contributing factors. Recent geophysical studies underscore the importance of advanced spatial modelling and precise evaluation of crustal dynamics for understanding regional deformation and mitigating risks in dynamic coastal environments (Eren, 2026). Geographic information systems (GIS) provide a powerful platform for managing, analysing, and visualising the diverse spatial data integral to such assessments (Siddiqui *et al*., 1996; Dai *et al*., 2001; Aly *et al*., 2005; Wang *et al*., 2009; Şener *et al*., 2010; Tudes and Yigiter, 2010; Youssef *et al*., 2011; Romano *et al*., 2015).

In order to achieve a comprehensive assessment, the spatial analysis in this study focuses on four key geophysical parameters that collectively determine seismic susceptibility. The primary indicators of susceptibility are proximity to fault lines, lithology, groundwater level, and slope. Proximity is a key factor in determining the level of susceptibility, with distance to fault lines being a crucial element in this regard. Lithology is another significant factor, as it dictates the local amplification of seismic waves. The influence of groundwater level on soil stability and liquefaction susceptibility is also a crucial factor in this regard. Finally, slope is a crucial geomorphological indicator of potential basin effects and seismic wave amplification in flat terrains. It is important to note that the groundwater level criterion itself represents a complex subsurface condition and was, therefore, derived from a secondary, more detailed analytic hierarchy process (AHP) model. The model under consideration incorporates a series of hydrogeological factors, including terrain morphology, fault density, land use, lithology, slope, soil depth, drainage density, and precipitation. The purpose of incorporating these factors is to

produce a robust spatial estimation of groundwater levels.

While GIS provide the platform for spatial analysis, a structured method is required to weigh the relative importance of the four primary criteria. Multi-criteria decision making (MCDM) methods have been developed for the purpose of evaluating and ranking alternatives in order to identify optimal solutions (Köksalan *et al*., 2011). For the purposes of this study, the AHP, developed by Saaty (1987), was selected over other MCDM techniques for several compelling reasons:

- this approach has been demonstrated to exhibit superior flexibility and substantial descriptive capacity;
- the system subject of discussion in this study is notable for its ability to restructure decision problems into hierarchical categories and to assign relative importance to each element;
- the present study validates the consistency of both objective and subjective assessments, thereby reducing potential biases in the decision-making process;
- the model has been demonstrated to be capable of effectively representing uncertainty and complex spatial susceptibility conditions. This is due to its capacity to derive ratio scales from pairwise comparisons (Tavana *et al*., 2023).

The capacity of AHP to integrate expert judgement with quantitative data has been proven. This makes it an invaluable tool for assigning priority weights to susceptibility parameters in a transparent and scientifically rigorous manner (Banai-Kashani, 1989; Vaidya and Kumar, 2006; Darko *et al*., 2019).

The objective of this study is to develop a comprehensive regional seismic susceptibility model for Bandırma and its environs by synergistically integrating GIS and AHP. The primary objective of this study was to generate a composite seismic susceptibility index (*SSI*) and a corresponding spatial zonation map, facilitating the classification of the study area into categories of relative seismic susceptibility. This research makes a significant contribution to the extant body of knowledge in this field by providing the first comprehensive, data-driven seismic susceptibility zonation specifically for the Bandırma region, thereby addressing a critical gap in local planning and disaster mitigation. Methodologically, it enhances the standard GIS-AHP approach through a hierarchical framework featuring a nested AHP model to derive the groundwater level parameter from multiple hydrogeological factors, providing a more explicit and traceable representation of this criterion. Furthermore, the study enhances methodological transparency by explicitly substantiating the classification thresholds employed for susceptibility factors in accordance with established geotechnical principles, and by examining the stability of the model outputs with respect to variations in the criteria weights through a sensitivity analysis. The work presented in this study constitutes a replicable framework and a tangible decision-support tool. The purpose of the framework and tool is to guide safer and more sustainable urban development practices in Bandırma and similar seismically active areas.

2. Methodology

The methodological framework of this study is designed to assess the regional seismic susceptibility in Bandırma and its environs. The methodology is founded upon the synergistic integration of GIS for spatial data processing and AHP for multi-criteria decision analysis. This approach facilitates the systematic evaluation of various geophysical factors and their synthesis into a comprehensive susceptibility index, thereby providing a robust decision-support tool for disaster mitigation and urban planning.

2.1. Study area

The geographical area under consideration comprises the city of Bandırma and its immediate environs, which are located in the Balıkesir province within the Marmara region of Turkey (Fig. 1). Bandırma is a significant coastal and port city on the southern coast of the Sea of Marmara. It is situated in a region of high seismic activity due to its proximity to active branches of the North Anatolian Fault. This geological context renders the area a critical one for seismic susceptibility assessment.

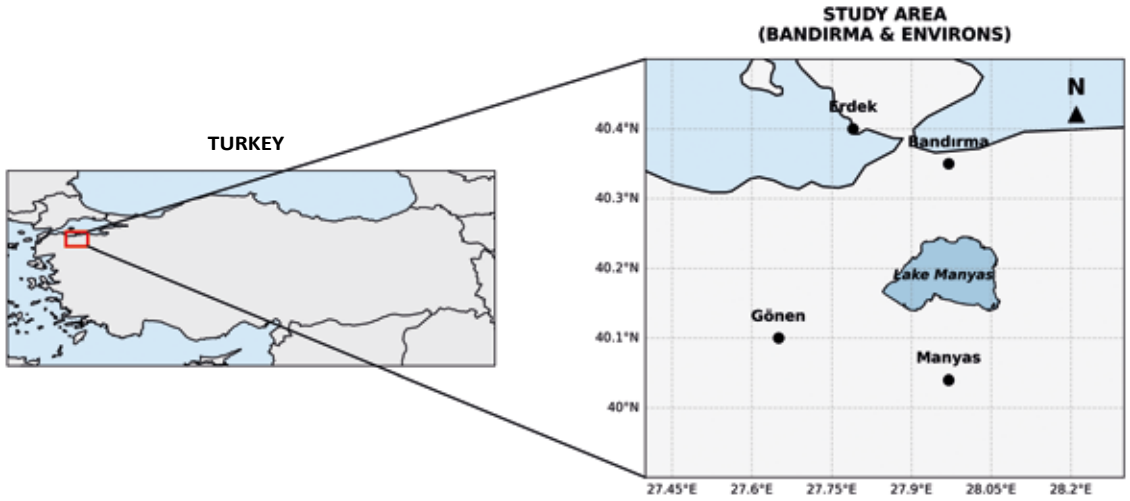


Fig. 1 - Location of the study area, Bandırma and its surroundings.

2.2. Data acquisition and pre-processing

The Shuttle Radar Topography Mission (SRTM) 1 Arc-Second Global Digital Elevation Model (DEM) was utilised as the fundamental topographic dataset for this study. This dataset was acquired from the NASA Earthdata Search portal and can be accessed via interfaces such as the ASF Data Search (2024). The DEM, with a spatial resolution of approximately 30 m, was obtained as three separate scenes covering the study extent. These scenes were, then, assembled into a single raster dataset by means of a bilinear interpolation method, thus ensuring smooth transitions between scenes. The base map was, then, projected to the Universal Transverse Mercator (UTM) Zone 35 North coordinate system, based on the WGS84 datum (EPSG:32635). Finally, the mosaicked and projected DEM was clipped precisely using the vector boundary polygon defining the research area. The processed DEM constituted the primary data source for deriving the slope map, employing the standard slope algorithm within the ArcGIS Spatial Analyst toolbox.

The additional thematic data layers were acquired and processed as follows:

- active fault lines: the most recent version (as of the study period) of the active fault map of Turkey was digitised from the publication by the General Directorate of Mineral Research and Exploration (MTA) of Turkey. Euclidian distance calculations were performed on this vector layer to generate the distance-to-fault raster;

- geology (lithology): the data was obtained from the official 1:100,000 scale digital geological maps provided by MTA. The relevant polygon features were extracted and rasterised to match the DEM resolution using the maximum area attribute assignment method;
- land use/land cover: derived from the CORINE Land Cover 2018 dataset, the raster was created using the cell centre assignment method. The primary function of this layer was as an input for the groundwater level sub-model.

All acquired vector and raster datasets were projected to the same UTM coordinate system (EPSG:32635). Raster datasets were resampled where necessary using the nearest neighbour method (for categorical data like lithology and land use) or bilinear interpolation (for continuous data, if alignment was needed beyond projection) to ensure identical cell size and spatial alignment before being used in the AHP weighting and overlay analysis. Standard raster processing tools were utilised within ArcGIS. Zonal statistics were not the primary tools for generating these input layers; however, they were employed for calculating area statistics for different classes within the final results.

2.3. Hierarchical framework for susceptibility assessment

A comprehensive review of the extant literature was conducted and a hierarchical model was subsequently formulated in order to structure the susceptibility assessment (Table 1). The model identifies four primary criteria that directly influence seismic susceptibility: The following factors were considered: distance to fault lines, lithology, groundwater level, and slope.

A fundamental element of this methodology is the utilisation of a nested, two-level AHP approach. While the four primary criteria were weighted at the first level to determine their overall influence on seismic susceptibility, the groundwater level criterion was itself a composite layer derived from a secondary AHP analysis. The secondary analysis incorporated eight hydrogeological and environmental factors, including geomorphology, fault density, land use, lithology, slope, soil depth, drainage density, and precipitation. In this hierarchical framework, lithology and slope serve dual, but physically distinct, functions. Within the secondary sub-model, they are evaluated strictly for their hydrogeological roles in governing groundwater accumulation and permeability. Conversely, in the primary susceptibility model, they are

Table 1 - Hierarchical framework of the GIS-AHP model for seismic susceptibility assessment.

Hierarchical level	**Criteria / parameters**
Level 1: goal	Seismic susceptibility potential
Level 2: primary criteria	1. Distance to fault lines 2. Lithology 3. Groundwater level 4. Slope
Level 3: sub-criteria (for groundwater level)	Parameters used to model groundwater level (Level 2, Criterion 3) - Geomorphology - Fault density - Land use - Lithology - Slope - Soil depth - Drainage Density - Precipitation

assessed independently for their direct geotechnical implications, specifically regarding seismic wave amplification and topographic basin effects. This hierarchical structure allows each factor to be represented according to the specific physical process it controls at the corresponding level of the model. It must, nevertheless, be acknowledged that, because lithology and slope contribute to the modelled groundwater layer and are subsequently reintroduced as independent criteria in the primary susceptibility model, part of their information content may enter the final index both directly and indirectly. The fact that the two levels describe different physical processes does not, by itself, establish statistical or functional independence, and a limited degree of partial dependence (or partial double counting) among the predictors cannot be excluded. This issue is discussed explicitly as a methodological limitation in Section 5.2.

2.4. GIS-based weighted overlay analysis

The final stage of the analysis entailed a weighted overlay operation, which was conducted utilising the spatial analyst tools in ArcGIS 10.8. In this final step, the thematic layers corresponding to the four primary criteria were reclassified based on their relative susceptibility contribution. The weights for each criterion, systematically derived from the AHP, were, then, applied to these reclassified layers. The GIS algorithm combined these weighted layers to produce the final seismic susceptibility map, which categorises the study area into zones of varying susceptibility potential.

3. Analysis of susceptibility factors

This section delineates the preparation and analysis of the four primary criteria that have been selected for the seismic susceptibility model. Each factor (distance to fault lines, lithology, slope, and groundwater level) was individually processed, reclassified into standardised susceptibility classes, and scored for the final AHP analysis. The subsequent subsections herein delineate the rationale and methodology applied to each criterion.

3.1. Fault lines and distances

In the field of seismic susceptibility assessment, the parameters of fault lines and distances are of critical importance. Proximity to an active fault directly influences the intensity of ground shaking and the potential for surface rupture (Kramer and Stewart, 2024). While distance to active faults is utilised herein as a spatial proxy for the relative intensity of expected shaking, it is explicitly acknowledged that this qualitative approach does not substitute for quantitative probabilistic or deterministic ground-motion estimations. Modern probabilistic seismic hazard assessments and ground-motion prediction models tailored for the Marmara region (Şeşetyan *et al*., 2019), as well as updated national seismic hazard frameworks (Akkar *et al*., 2018), are essential for deriving these rigorous quantitative metrics. Therefore, the distance-based classification employed in this study serves strictly as a macro-level indicator. Seismic energy attenuates rapidly with distance from the source, necessitating the reclassification of continuous distance data into discrete susceptibility zones for multi-criteria evaluation models such as the AHP.

The Bandırma district is under significant potential threat from three primary fault systems related to the North Anatolian Fault zone. The recent seismic activity along these faults underscores their potential influence on regional susceptibility. In the course of this study,

the distance-to-fault layer was subjected to reclassification, with the result that it was divided into five susceptibility categories (Table 2). The selection of thresholds and the allocation of susceptibility scores (ranging from 1, indicating minimal susceptibility, to 5, denoting maximal susceptibility) are in accordance with prevailing methodologies in regional seismic susceptibility zonation studies and are in alignment with the tenets of seismic wave attenuation (Aghataher *et al*., 2008; Panahi *et al*., 2014).

To elaborate further:

- the highest susceptibility score (5) was assigned to the immediate vicinity (0–500 m), representing the zone with the highest potential for surface rupture and maximum ground acceleration. This zone is often considered the near-field source zone where the potential for severe site effects is greatest;
- the subsequent buffer zones (501–1,000 m and 1,001–2,000 m, scores 4 and 3) represent areas where significant ground shaking is still expected, albeit with attenuation. The 2 km threshold is frequently regarded as a critical boundary, characterised by severe near-field effects for moderate-to-large earthquakes in analogous tectonic settings (Panahi *et al*., 2014);
- the wider buffer zones (2,001–5,000 m and >5,000 m, scores 2 and 1) reflect areas where ground shaking intensity is expected to be substantially lower due to geometric spreading and anelastic attenuation, transitioning towards far-field effects (Kramer and Stewart, 2024). Although absolute safety cannot be guaranteed even at these distances, the relative susceptibility is significantly reduced in comparison to areas in closer proximity to the source.

This classification scheme draws parallels with methodologies employed in studies such as those by Aghataher *et al*. (2008) and Panahi *et al*. (2014). However, it is fundamentally reliant on the physical principle. It has been demonstrated that the seismic susceptibility decreases nonlinearly with distance from the causative fault.

A quantitative analysis based on this classification (Table 2) reveals the distribution of susceptibility across the study area. A total area of 14,782 hectares, constituting 6.07% of the region, is classified as ‘very high’ susceptibility (0–500 m). Cumulatively, areas within 2 km of a fault line (very high, high, and moderate susceptibility) account for approximately 23.78% of the study area. The largest portion of the area, categorised as ‘very low’ susceptibility (>5,000 m), encompasses 49.10% (119,437 Ha). The spatial distribution is shown in Fig. 2.

3.2. Lithology

The lithological composition of the near-surface geology is a fundamental parameter governing the spatial distribution of seismic susceptibility, primarily through the phenomenon

Table 2 - Reclassification of fault distances, assigned susceptibility scores, and area distribution.

Distance to fault (m)	Susceptibility score	Susceptibility category	Area (Ha)	Percentage (%)
0 – 500	5	Very high	14,782	6.07
501 – 1,000	4	High	14,025	5.76
1,001 – 2,000	3	Moderate	29,084	11.95
2,001 – 5,000	2	Low	65,988	27.12
>5,000	1	Very low	119,437	49.10
Total			**243,316**	**100.00**

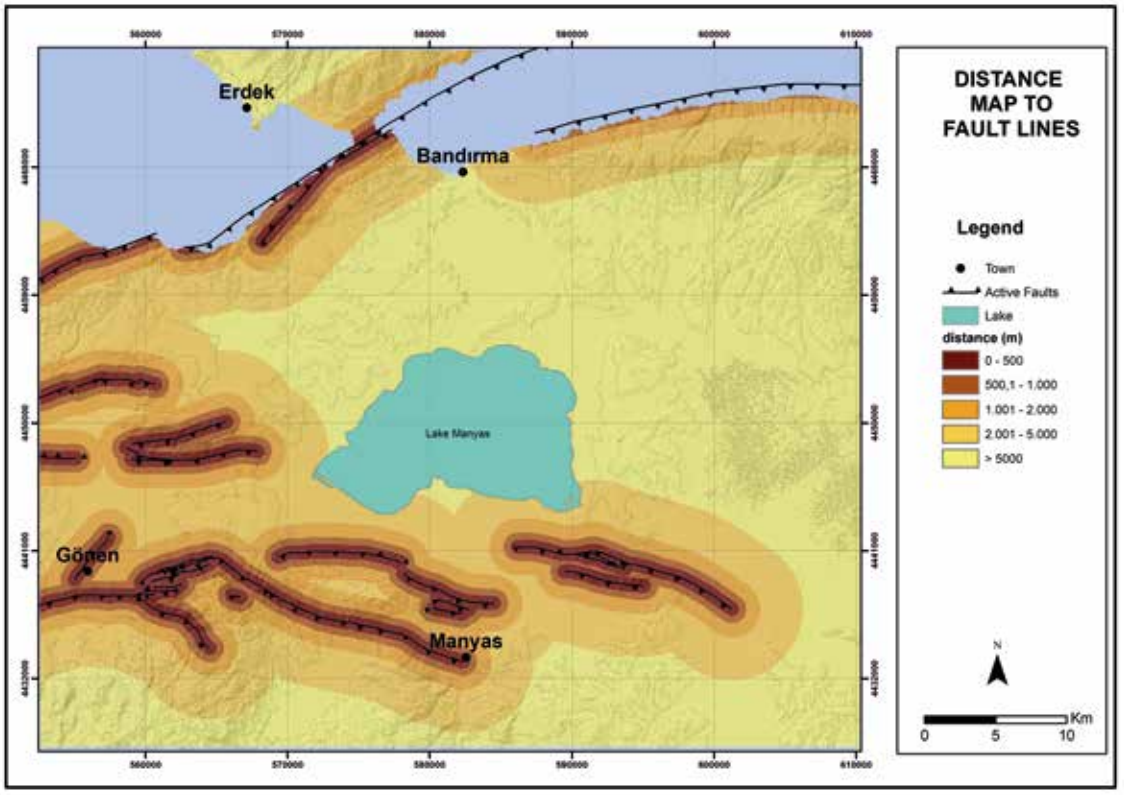


Fig. 2 – Map of distance to fault lines of the study area, reclassified into susceptibility zones.

of site effects. This refers to the modification of seismic wave characteristics as they propagate from deeper, competent bedrock to the ground surface through softer soil layers (Kramer and Stewart, 2024). The engineering properties of these superficial materials, particularly their shear wave velocity (V_S) and their potential for nonlinear behaviour, dictate their response to seismic loading and the resulting intensity of ground shaking experienced by structures.

The fundamental lithological data for this study were obtained from the 1:100,000 scale digital geological maps provided by the MTA. The map units were subjected to digitisation and processing within a GIS environment. In order to undertake a susceptibility-based AHP analysis, it was necessary to reclassify each lithological unit into one of five susceptibility categories (Table 3).

The assignment of susceptibility scores was based on well-established principles of engineering geology and seismology. While detailed V_{S30} mapping and *in-situ* soil classification are strictly required for precise seismic site effect evaluation and ground-motion amplification modelling (Kanlı *et al*., 2006), such high-resolution instrumental microzonation is beyond the scope of this regional study. Consistent with the macro-scale of this assessment, the classification relies on broad geological categories rather than site-specific V_{S30} field measurements or instrumental microzonation studies. Consequently, the derived qualitative ranking functions as a preliminary spatial screening tool rather than a definitive site-response analysis. In particular, the correlation of lithological descriptions with expected geotechnical performance under seismic loading was considered, with typical V_{S30} ranges associated with these materials in seismic site classification systems being of particular relevance (Kramer and Stewart, 2024):

- score 5 (very high susceptibility). The subject has been assigned to unconsolidated recent Quaternary deposits, such as alluvium and water bodies. These materials typically correspond to the National Earthquake Hazards Reduction Program (NEHRP) site Class E or F, exhibiting very low shear wave velocities (V_S often < 180 m/s), leading to significant ground motion amplification. Furthermore, when saturated, they demonstrate a high potential for liquefaction, thereby constituting a grave threat to foundation stability (Seed and Idriss, 1971);
- score 4 (high susceptibility). Alluvial cone deposits are classified under this category. Although these deposits are unconsolidated, they may exhibit slightly higher density or coarser grain sizes compared to floodplain alluvium, which is commonly classified as site Class D or E. Consequently, their seismic performance may be marginally better; however, they still present a high susceptibility to ground motion amplification and liquefaction relative to rock sites;
- score 3 (moderate susceptibility). The mineralogical composition of the sedimentary rocks in question has been determined to be limestone, sandstone, and coal. These units are typically commensurate with NEHRP site Class C or D, exhibiting greater competence in comparison to recent sediments, though demonstrating variability in cementation and fracturing. Typically, these units exhibit moderate V_S values and comparatively diminished amplification potential in comparison to score 4 and 5 units. Nonetheless, these values remain significantly higher than those observed in competent bedrock;
- score 2 (low susceptibility). The mineral is found in metamorphic rocks of the schist variety. These rocks are typically competent, yet they exhibit foliation, a structural feature that can influence wave propagation. Their seismic performance is typically superior to that of sedimentary rocks but potentially less favourable than that of massive igneous or high-grade metamorphic rocks, which often fall into Class C or B/C.
- score 1 (very low susceptibility). The following rocks have been assigned to this category:
  - igneous rocks that are competent (e.g. andesite, basalt, granodiorite, pyroclastic rock, metavolcanic);
  - metamorphic rocks that are high-grade (e.g. marble);
  - tectonic units that are complex (e.g. melange, which often contains competent blocks). These units are typically indicative of bedrock conditions that correspond to NEHRP site Class B or A, characterised by high V_S (>760 m/s), leading to negligible ground motion amplification and serving as a reference 'firm ground' condition.

This scoring is indicative of a standard qualitative ranking, the basis of which is the expected amplification behaviour and stability under seismic loads. These principles have been outlined in the relevant geotechnical earthquake engineering literature (Kramer and Stewart, 2024).

Table 3 details the susceptibility scores and area distribution. Units exhibiting elevated seismic susceptibility (scores 3–5) predominate, with sandstone (31.48%) and alluvium (29.59%) being the most prevalent. Competent bedrock units, categorised as 'very low susceptibility' with a score of 1, account for a significantly smaller percentage of the total. The spatial distribution is illustrated in Fig. 3.

3.3. Slope

Topographic slope is considered an important indicator of seismic susceptibility, primarily because it correlates strongly with local site conditions, near-surface shear-wave velocity, and basin amplification. As demonstrated by Wald and Allen (2007), in seismically active regions,

Table 3 - Reclassification of lithological units, assigned susceptibility scores, and area distribution.

Lithological unit	Susceptibility score	Area (Ha)	Percentage (%)
Marble	1	3,803	1.56
Limestone	3	1,793	0.74
Alluvium	5	71,993	29.59
Andesite basalt	1	18,900	7.77
Schist	2	31,152	12.80
Sandstone	3	76,591	31.48
Granodiorite	1	4,041	1.66
Pyroclastic rock	1	1,206	0.50
Melange	1	421	0.17
Culm	3	16,638	6.84
Metavolcanic	1	493	0.20
Water bodies	5	16,239	6.67
Alluvial cone	4	45	0.02
Total		**243,316**	**100.00**

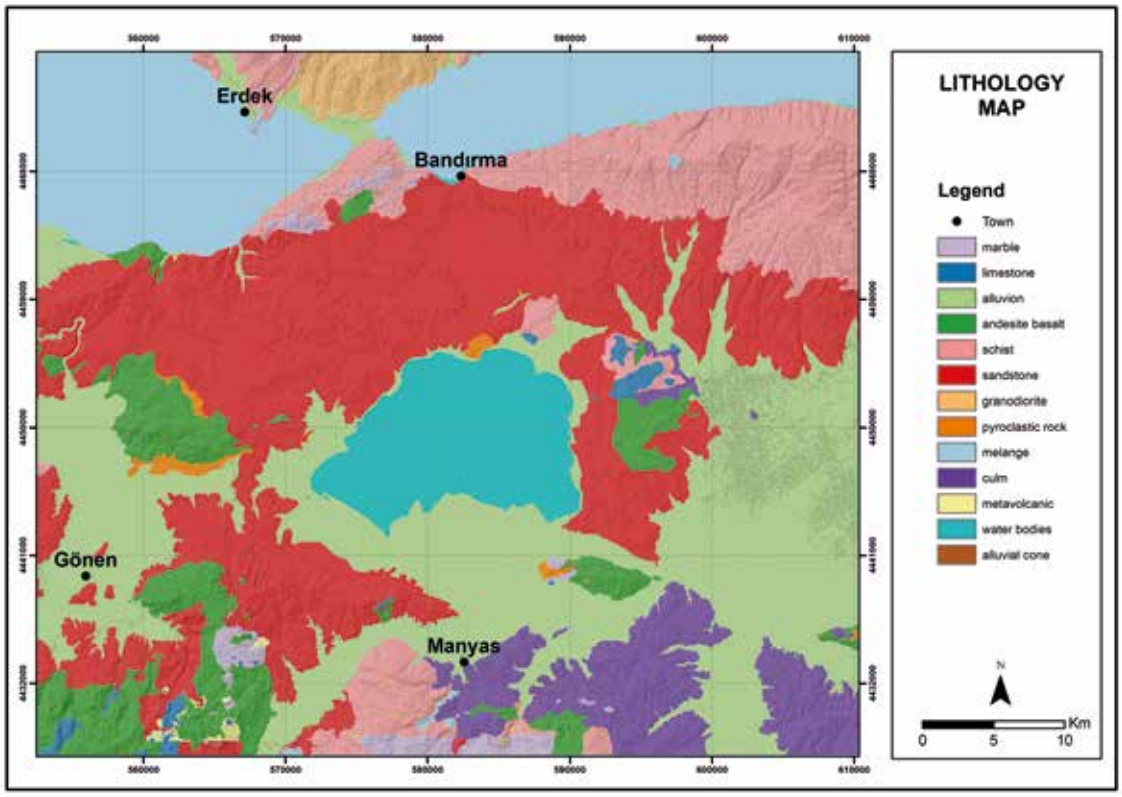


Fig. 3 - Lithological map of the study area (data source: MTA).

topographic slope has been shown to provide a reliable proxy for estimating seismic site conditions. Flat and gently sloping terrains (0–10%) typically correspond to deep sedimentary basins, valleys, and alluvial plains. These flat morphological depressions are composed of finer,

unconsolidated sediments with low shear-wave velocities, which may increase the potential for seismic wave amplification and liquefaction. Conversely, steep mountainous terrains (>20%) generally consist of outcropping competent bedrock that resists weathering and maintains higher shear velocities, thereby generally exhibiting lower levels of ground-motion amplification and providing greater dynamic stability against shaking.

The slope map for the study area was derived from the DEM using the Spatial Analyst tools in ArcGIS. The resulting continuous slope data, measured in percentages, were reclassified into five distinct susceptibility categories to facilitate the AHP modelling framework. Consistent with the geo-environmental evaluation approach proposed by Dai *et al*. (2001), these categories were assigned susceptibility scores based on the potential for topographic basin amplification and its inverse relationship with shear-wave velocity. As outlined in Table 4, the highest susceptibility score (5) was allocated to the flattest areas (0–5%), reflecting the higher amplification potential associated with plain and basin morphologies, while the lowest score (1) was assigned to the steepest terrain (>20%), representing the relative stability of hard-rock formations against seismic ground acceleration.

A quantitative analysis of the slope distribution (Table 4), based on the map presented in Fig. 4, reveals that the study area is predominantly characterised by topography exhibiting characteristics typical of basins prone to wave amplification. A total of 43.56% (105,963 hectares) of the region is classified as 'very high' susceptibility strictly in terms of topographic slope, representing the flat plains (0–5%). In combination with the 'high' susceptibility class (5.01–10% slope, covering 23.35% or 56,820 ha), the analysis shows that over two-thirds (66.91%) of the landscape is composed of flat to gently sloping terrain, suggesting a high potential for seismic-wave amplification. Conversely, areas with relatively low amplification potential due to steep slopes (greater than 20%, designated as 'very low' susceptibility) constitute 14.42% (35,092 hectares) of the region, primarily concentrated in highland areas. The spatial distribution of the aforementioned susceptibility classes is illustrated in Fig. 4.

Table 4 - Reclassification of slope values, assigned susceptibility scores, and area distribution.

Slope class (%)	Susceptibility score	Area (Ha)	Percentage (%)
0-5	5	105,963	43.56
5.01 - 10	4	56,820	23.35
10.01 - 15	3	26,797	11.01
15.01 -20	2	18,645	7.66
> 20	1	35,092	14.42
Total		**243,316**	**100.00**

3.4. Groundwater level

The groundwater level is a pivotal factor in seismic susceptibility assessment, as it directly influences two critical failure mechanisms: soil liquefaction and the reduction of soil bearing capacity. In soils with high water content and low cohesion, such as saturated, unconsolidated granular soils, the propagation of seismic waves can result in a rapid increase in pore water pressure. This increase can cause the soil to lose its strength and behave like a liquid. This phenomenon is known as liquefaction (Seed and Idriss, 1971).

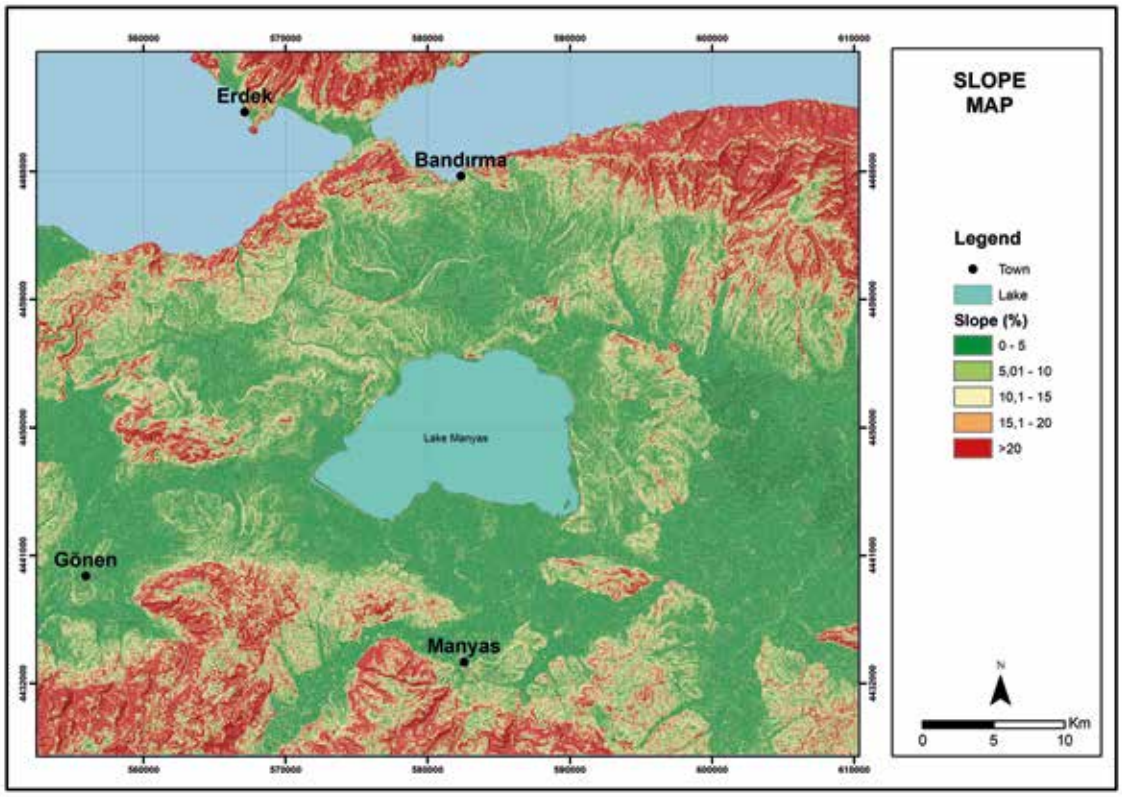


Fig. 4 - Slope map of the study area, classified into five susceptibility categories.

In view of the impracticality of conducting direct, widespread field measurements and the general scarcity of continuous regional piezometric data, the groundwater level for the study area was modelled using a secondary, nested AHP model. This approach integrates eight key hydrogeological and environmental parameters to influence groundwater conditions. The integration of such environmental variables within a GIS framework is widely recognised as a reliable spatial proxy for estimating relative groundwater accumulation in regions lacking dense monitoring networks (Jha *et al*., 2007). The relative influence of each parameter was determined through pairwise comparisons by applying established hydrogeological principles from the literature to the specific conditions of the study area. The resulting Consistency Ratio (CR) of 0.08, which is below the acceptable threshold of 0.10, confirms the logical consistency of these judgments. The final normalised weights, as outlined in Table 5, demonstrate that geomorphology (24.18%) and fault density (18.64%) were the most significant factors in the model. The integration of these weighted layers was subsequently undertaken using a weighted overlay tool in ArcGIS, thereby yielding the final groundwater level potential map.

The model's output indicates that a significant proportion of the study area is characterised by a shallow groundwater table (Fig. 5). The largest single category is that of areas classified as having a 'high' groundwater level, which constitutes 43.72% of the region. When combined with areas of 'moderate' groundwater level (30.08%), it becomes evident that nearly three-quarters of the landscape exhibits conditions that could potentially increase seismic susceptibility.

For the primary seismic susceptibility assessment, the final modelled groundwater map was reclassified into five susceptibility categories. As demonstrated in Table 6, a direct correlation

Table 5 - Normalised weights of the parameters used in the AHP model for groundwater level.

Parameter	Weight	Percentage (%)
Geomorphology	0.24	24.18
Fault density	0.19	18.64
Land use	0.18	18.40
Lithology	0.11	10.91
Slope	0.10	10.07
Soil depth	0.07	6.77
Drainage density	0.07	6.71
Precipitation	0.04	4.33
Total	**1.00**	**100.00**

was identified, whereby an elevated groundwater table was assigned a higher susceptibility score. This classification is predicated on the increased potential for liquefaction and reduced soil stability under seismic loading, as established in foundational geotechnical earthquake engineering principles (Seed and Idriss, 1971).

Table 6 - Reclassification of the modelled groundwater level and its assigned susceptibility score.

Groundwater level	Susceptibility score	Rationale / Justification
Very low	1 (very low)	Deep groundwater table; negligible liquefaction potential.
Low	2 (low)	Low liquefaction potential; minimal impact on soil stability.
Moderate	3 (moderate)	Moderate liquefaction susceptibility under strong shaking; potential for some stability loss.
High	4 (high)	High liquefaction susceptibility in vulnerable soils; significant reduction in bearing capacity.
Very high	5 (very high)	Very high and widespread liquefaction potential; severe threat to foundation stability.

4. AHP-based susceptibility analysis and results

Subsequent to the establishment of the methodological framework, the core analysis was conducted in two stages. Initially, the AHP was utilised to ascertain the weights of the four primary susceptibility criteria. Secondly, these weights were applied within a GIS environment to generate the final seismic susceptibility map and quantify the resulting susceptibility zones.

4.1. Weighting of primary criteria

The four primary criteria identified in the methodology (distance to fault lines, lithology, groundwater level, and slope) were weighted in order to ascertain their relative influence on overall seismic susceptibility. To improve the transparency and reproducibility of the weighting procedure, the pairwise comparisons were derived from a systematic synthesis of established GIS-AHP seismic susceptibility studies conducted in similar seismotectonically active regions (Erden and Karaman, 2012; Değerliyurt, 2014; Panahi *et al*., 2014).

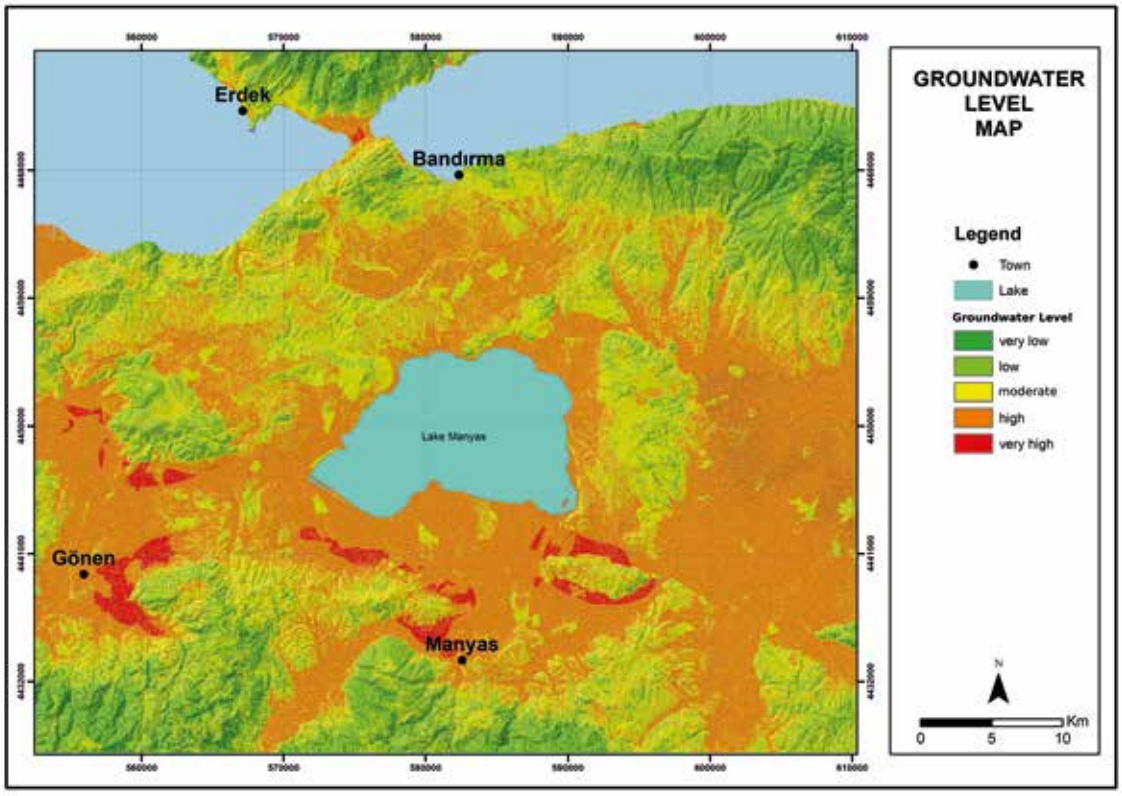


Fig. 5 - Final modelled groundwater level map of the study area.

The rationale behind this hierarchical weighting scheme follows the ordering commonly adopted in previous GIS-AHP susceptibility studies and in the general geotechnical literature:

- distance to fault lines: proximity to seismogenic sources dictates the primary input of seismic energy, rendering it the most dominant factor. This aligns with the multidisciplinary consensus reported by Erden and Karaman (2012), who assigned a paramount weight (38.0%) to this parameter;
- lithology: closely follows fault proximity, as it governs the immediate site response and structural wave amplification. This is consistent with the established importance of near-surface soil classification in regional macro-zonation models;
- groundwater and slope: while critical for secondary failure mechanisms such as liquefaction and topographic basin effects, respectively, these act as compounding modifiers rather than primary source drivers (Değerliyurt, 2014). Consequently, they are assigned comparatively lower relative weights.

The pairwise comparison matrix for the primary criteria, ensuring mathematical reciprocity, is presented in Table 7. The relative importance of each criterion is quantified by this matrix against the others, based on the Saaty (1987) nine-point scale.

The matrix was subsequently subjected to a process of normalisation, after which the priority vector, representing the final weights for each criterion, was calculated by means of the eigenvector method. The reliability of the judgments was confirmed by calculating the CR. The resulting CR value was found to be approximately 0.006, which is well below the 0.10 threshold, indicating that the synthesised judgements form an internally consistent matrix. It should be

Table 7 - Corrected pairwise comparison matrix for the Level 2 primary criteria.

Criterion	Dist. to fault (a)	Lithology (b)	Groundwater (c)	Slope (d)
Dist. to fault (a)	1	1	2	3
Lithology (b)	1/2	1	2	2
Groundwater (c)	1/2	1/2	1	1
Slope (d)	1/3	1/2	1	1

noted that the CR evaluates only the logical coherence of the pairwise comparisons and provides no measure of the physical accuracy of the assigned weights.

The final derived weights are presented in Table 8. The calculated weights for distance to fault lines (0.380) and lithology (0.288) are comparable to the values reported in previous GIS-AHP studies conducted in similar seismotectonic settings, and the remaining criteria follow the same relative ordering: groundwater level (0.176) and slope (0.156). This agreement indicates that the adopted scheme is consistent with existing expert- and literature-based weighting approaches; it does not demonstrate that the weights are physically validated, intrinsically accurate, or optimal for the specific conditions of Bandırma. As acknowledged in Section 5.2, AHP weighting inevitably retains a degree of expert-based judgement, and the resulting hierarchy should, therefore, be regarded as a transparent and reproducible, but still partly subjective, prioritisation scheme.

Table 8 - Recalculated final weights of the primary criteria.

Criterion	Calculated weight	Percentage
Distance to fault (a)	0.380	38.0%
Lithology (b)	0.288	28.8%
Groundwater level (c)	0.176	17.6%
Slope (d)	0.156	15.6%
Total	**1.000**	**100.0%**

4.2. Final susceptibility map and zonation results

The final seismic susceptibility map was generated by integrating the four criteria layers in ArcGIS 10.8 using the Weighted Overlay tool. Initially, each criterion's sub-classes were reclassified onto a standardised susceptibility scale ranging from 1 (very low susceptibility) to 5 (very high susceptibility).

The final *SSI* for each pixel was, then, calculated using the newly derived weights from the AHP (Table 8) according to the following updated formula:

$$SSI = \left(0.380 x P_{fault}\right) + \left(0.288 x P_{litho}\right) + \left(0.176 x P_{gw}\right) + \left(0.156 x P_{slope}\right) \quad (1)$$

where *P* represents the reclassified susceptibility score (1-5) for each parameter.

The resulting continuous *SSI* map was, then, classified into five discrete susceptibility zones: the scale ranges from very low to very high (Fig. 6). The spatial distribution and proportional allocation of these susceptibility zones are delineated in Table 9.

Table 9 - Area distribution of the final seismic susceptibility zones.

Susceptibility category	Susceptibility score	Area (Ha)	Percentage (%)
Very low	1	30,444	12.51
Low	2	103,738	42.63
Moderate	3	67,869	27.89
High	4	35,128	14.44
Very high	5	6,137	2.52
Total		**243,316**	**100.00**

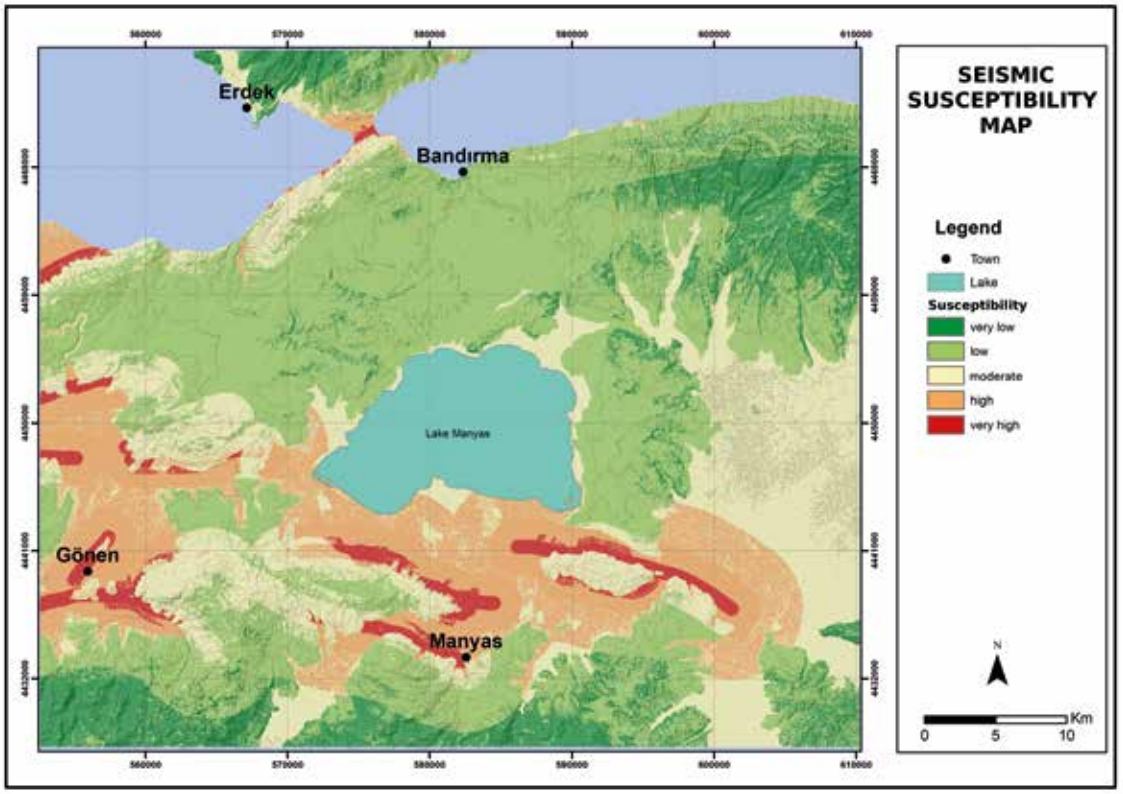


Fig. 6 - Final seismic susceptibility map of the study area.

The results indicate that the majority of the study area (42.63%) is classified as 'low' susceptibility. However, a considerable proportion of the data falls into the 'moderate' (27.89%) and 'high' (14.44%) susceptibility categories. A total of 6,137 hectares (2.52%) of the study area is classified in the 'very high' susceptibility category. As illustrated in Fig. 6, these high susceptibility areas are characterised by a combination of factors, including proximity to fault lines, unfavourable lithology (such as alluvium), and high groundwater levels. These areas should, therefore, be prioritised for detailed site-specific investigation and considered in subsequent land-use planning and mitigation studies.

5. Discussion

The present study successfully developed and implemented an integrated GIS-AHP model to generate a seismic susceptibility map for Bandırma and its environs. The quantitative results, which categorise 2.52% of the area as 'very high' susceptibility and 14.44% as 'high' susceptibility (Table 9), provide a spatial overview of the relative seismic susceptibility of the region. The spatial distribution of these high-susceptibility zones, as visualised in the final susceptibility map (Fig. 6), is not arbitrary. This finding directly corresponds to the criteria identified as most critical in the AHP model. The 'very high' susceptibility zones are predominantly concentrated along the active fault lines that traverse the southern part of the study area (near Gönen and Manyas) and in the coastal plains. This clustering is a direct consequence of the high weights assigned to 'Distance to fault lines' (38.0%) and 'Lithology' (28.8%) (Table 8). These high-susceptibility areas almost perfectly overlap with zones of unconsolidated alluvium and close fault proximity, a combination which is known to dramatically amplify seismic shaking and increase liquefaction potential.

In order to place the resulting zonation in context, a qualitative benchmarking exercise was carried out by cross-referencing the high-susceptibility zones with the official national seismic hazard data (AFAD, 2018) and with regional historical earthquake damage reports. The 'very high' susceptibility zones identified in this study show a broad spatial correspondence with the high-hazard regions delineated in the national seismic hazard mapping, and they also fall within areas that have historically experienced pronounced ground-shaking effects in the Marmara region. This comparison must, however, be interpreted with caution, and it does not constitute an independent validation of the model or a demonstration of its predictive reliability. A certain degree of agreement with the national seismic hazard maps is to be expected, because distance to active faults is the most heavily weighted criterion in the present model and is also a primary control on the national hazard estimates. Likewise, historical damage distributions are governed not only by local ground conditions, but also by the characteristics of the causative earthquakes, exposure, structural vulnerability, building quality, and construction practice, none of which is explicitly represented in the present framework. The exercise reported here is, therefore, more appropriately described as a qualitative benchmarking and consistency check than as an empirical validation in a strict sense. As stated in Section 5.2, a rigorous validation would require calibration against instrumental ground-motion records, systematic field observations, and documented liquefaction inventories.

To contextualise these findings and evaluate the regional scientific contribution of this study, it is crucial to benchmark the susceptibility distribution of Bandırma with similar seismotectonically active coastal cities. For instance, studies conducted in the Küçükçekmece region of Istanbul (Erden and Karaman, 2012) and Iskenderun (Değerliyurt, 2014) similarly identified unconsolidated Quaternary deposits and near-field fault zones as the primary drivers of seismic susceptibility. However, the quantitative analysis reveals a distinct spatial configuration for Bandırma. Unlike broader coastal plains where high susceptibility is often uniformly distributed, Bandırma's 'high' and 'very high' susceptibility zones (cumulatively 16.96%) are highly localised. They are heavily constrained by the specific intersection of shallow groundwater accumulations (modelled via the 8-parameter sub-AHP) and the immediate deformation zones of the North Anatolian Fault branches. While it is geophysically expected that alluvium and fault proximity yield high susceptibility, the scientific novelty presented in this study lies in the spatial quantification of these overlapping susceptibility conditions.

The efficacy of the GIS-AHP integration itself is also reinforced. The present application of the methodology is consistent with a considerable number of international studies that have

validated its robustness for land-use suitability and susceptibility assessment. This confirms its utility as a transparent and effective decision-support tool (Tudes and Yigiter, 2010; Panahi *et al*., 2014; Romano *et al*., 2015).

Furthermore, the study's most notable strength is its utilisation of a hierarchical, nested AHP approach for the 'Groundwater level' criterion (Table 1). While many regional studies rely on generalised assumptions or sparse well data for liquefaction potential, this parameter was modelled as a composite of eight distinct hydrogeological factors. This approach provides a more spatially detailed and traceable estimate of relative groundwater conditions than generalised assumptions or sparse well data enable, which may support preliminary screening for local urban planning and disaster mitigation.

5.1. Sensitivity analysis

In order to evaluate the robustness of the final seismic susceptibility zonation map to variations in the AHP-derived weights, a sensitivity analysis was performed. This analysis assesses how potential changes in the relative importance assigned to the primary criteria might affect the spatial distribution and extent of the calculated susceptibility zones. The One-At-A-Time approach was adopted, whereby the weight of each primary criterion was individually increased and decreased by 10%, with the weights of the remaining criteria proportionally adjusted to maintain a total sum of 1.0. For each of the scenarios under consideration, the resulting shifts in the percentage area of each susceptibility zone were visualised through a heatmap (Fig. 7). This graphical representation enables an immediate assessment of the model's response to weight fluctuations.

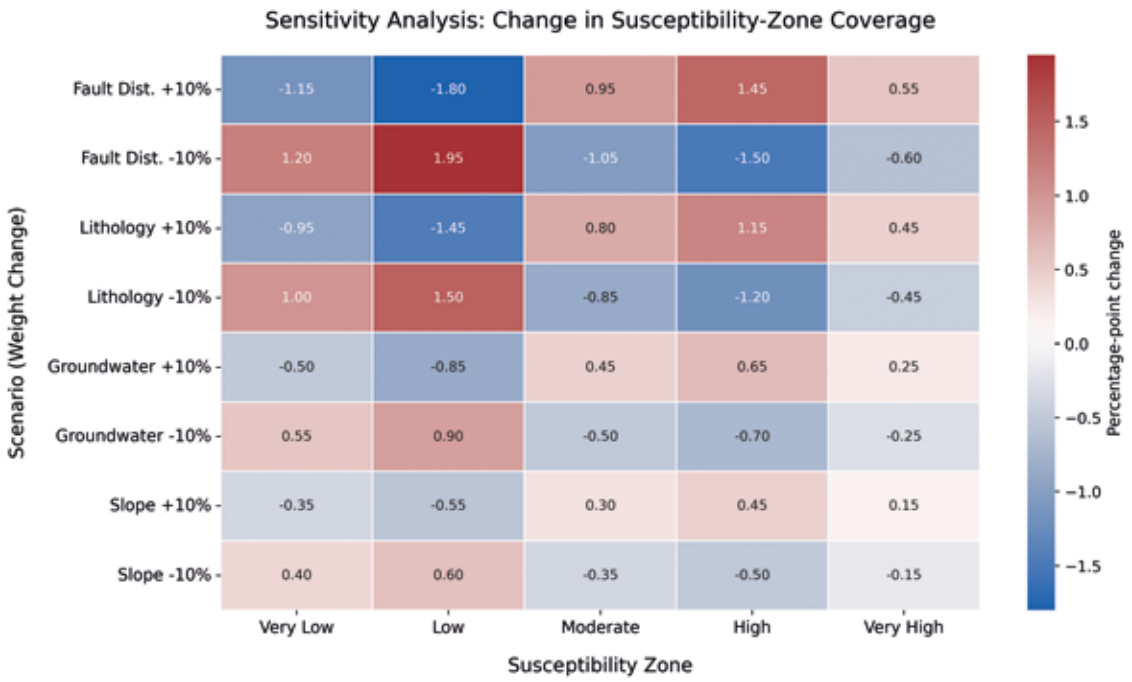


Fig. 7 - Sensitivity analysis heatmap showing the impact of criteria weight fluctuations on the spatial distribution of the seismic susceptibility categories.

The sensitivity analysis indicates that the model exhibits reasonable robustness. As anticipated, and as clearly illustrated by the colour intensities in Fig. 7, variations in the weights of the most influential criteria, 'Distance to fault lines' and 'Lithology', resulted in the most significant shifts in susceptibility zone areas. However, even a change of up to 10 percentage points in these dominant weights resulted in relatively minor absolute changes in the area covered by each susceptibility category. It was observed that alterations in the weights of 'Groundwater level' and, in particular, 'Slope' exerted a significantly diminished effect. The diverging colour scale in the heatmap further confirms that the primary spatial pattern of high-susceptibility zones, characterised by their concentration near faults and on soft soils, remained consistent across all scenarios. This finding indicates that, although adjustments to the weights can shift the classification boundaries, the spatial delineation of the most susceptible areas remains stable under the perturbations tested. It should be emphasised that the sensitivity analysis demonstrates stability with respect to these specific weighting variations only; it does not establish the accuracy or the predictive validity of the model.

5.2. Limitations and future work

While the proposed methodology provides a systematic framework for regional-scale seismic susceptibility assessment, the present study has several limitations inherent to macro-zonation approaches. The primary limitation is related to the spatial resolution of the input datasets, particularly the 30 m DEM. Although this resolution is suitable for regional-scale assessments, it may not adequately represent local-scale variations required for site-specific microzonation and engineering applications. Therefore, future studies should focus on integrating higher-resolution datasets, including LiDAR-derived elevation models, detailed geological information, and comprehensive geotechnical investigation data.

In addition, although the AHP-based weighting scheme was developed through a systematic synthesis of previous studies to improve methodological consistency, the approach still involves a degree of expert-based judgment. Future research should incorporate sensitivity and uncertainty analyses to evaluate the influence of weighting variability on susceptibility outcomes. Furthermore, calibration of the susceptibility model using instrumental ground-motion records, field observations, and documented liquefaction inventories would improve the reliability and transferability of the proposed framework.

A further methodological limitation concerns the potential dependence among the selected criteria. Lithology and slope are used both as inputs to the nested groundwater sub-model and as independent criteria in the primary susceptibility model. Although these two uses correspond to different physical roles, namely the hydrogeological control of groundwater accumulation and permeability on the one hand and seismic site response and topographic basin effects on the other, this conceptual distinction does not guarantee statistical or functional independence. Consequently, part of the information carried by these layers may be represented twice in the final susceptibility index, and a limited degree of double counting cannot be ruled out. Future work should, therefore, examine the correlation and dependence structure among the predictors, for example through correlation analysis, variance inflation diagnostics, or principal component-based reformulations, and should test alternative model structures in which the groundwater layer is derived exclusively from variables that are not reused at the primary level, in order to quantify the influence of this dependence on the resulting susceptibility patterns.

Despite these limitations, the generated susceptibility map represents a useful spatial decision-support tool for urban planning and risk-informed management in Bandırma. The

areas, classified as having 'high' and 'very high' susceptibility, should be prioritised for detailed investigation. Future urban development in these zones should be supported by site-specific geotechnical assessments and compliance with appropriate seismic design regulations to reduce the potential impacts indicated by this macro-scale assessment.

6. Conclusions

The objective of this study was to develop a comprehensive, spatially explicit seismic susceptibility model for Bandırma and its environs by synergistically integrating GIS and the AHP. The study successfully achieved this objective, culminating in the creation of a susceptibility zonation map that classifies the entire region into five distinct susceptibility categories.

The model identified that 16.96% of the study area (41,265 hectares) falls into 'high' or 'very high' susceptibility categories. The AHP analysis, which is based on a systematic synthesis of the literature and shows a high degree of internal consistency (CR = 0.006), indicates that 'Distance to fault lines' (38.0%) and 'Lithology' (28.8%) are the most influential criteria within the adopted weighting scheme.

The present study makes several significant contributions to the field. Firstly, it delivers the first holistic, data-driven seismic susceptibility assessment specifically for the vulnerable Bandırma region, identifying and quantifying high-susceptibility zones previously unmapped at this scale. Secondly, it develops the standard GIS-AHP approach through a nested AHP model for the groundwater criterion and an explicit justification of the reclassification thresholds, thereby improving methodological transparency and reproducibility. Thirdly, the sensitivity analysis shows that the resulting zonation is stable with respect to the weighting variations tested, although it does not by itself establish the accuracy or the predictive validity of the model. In conclusion, the study provides a replicable framework and a preliminary decision-support tool for local authorities. The results may assist urban planners and civil engineers in Bandırma in regional-scale screening and in prioritising the areas in which further investigation is required; they should not, however, be interpreted as definitive engineering or planning information, and site-specific geotechnical and seismological investigations remain necessary before any design, regulatory or site-selection application. It is recommended that future research efforts concentrate on the refinement of the regional model under consideration through the implementation of microzonation studies, utilising data with a higher resolution.

Acknowledgments. The author wishes to express their sincere gratitude to the General Directorate of Mineral Research and Exploration (MTA) of Turkey for providing the essential geological data used in this study. The author also thanks the Scientific Research Projects Coordination Unit of Fırat University (FÜBAP) for their valuable support. Additionally, the author acknowledges the utilisation of the Google Gemini language model during the preparation of this manuscript for the purpose of language editing and formatting. This study was financially supported by the Scientific Research Projects Coordination Unit of Fırat University (FÜBAP) under Project No. TEKF.25.74. The datasets generated and analysed during the current study are available from the corresponding author on reasonable request. Geological data supporting the findings of this study were obtained from the General Directorate of MTA.

REFERENCES

AFAD (Disaster and Emergency Management Presidency); 2018: *Earthquake hazard map of Turkey*. https://tdth.afad.gov.tr/, accessed 15 February 2026.

Aghataher R., Delavar M.R., Nami M.H. and Samnay N.; 2008: *A fuzzy-AHP decision support system for evaluation of cities vulnerability against earthquakes*. World Appl. Sci. J., 3, 66-72.

Akkar S., Azak T., Çan T., Çeken U., Demircioğlu Tümsa M.B., Duman T.Y., Erdik M., Ergintav S., Kadirioğlu F.T., Kalafat D., Kale Ö., Kartal R.F., Kekovalı K., Kılıç T., Özalp S., Altuncu Poyraz S., Şeşetyan K., Tekin S., Yakut A., Yılmaz M.T., Yücemen M.S. and Zülfikar Ö.; 2018: *Evolution of seismic hazard maps in Turkey*. Bull. Earthquake Eng., 16, 3197-3228, doi: 10.1007/s10518-018-0349-1.

Alonso W.; 1964: *Location and land use: toward a general theory of land rent*. Harvard University Press, Cambridge, MA, U.S.A., 204 pp., doi: 10.4159/harvard.9780674730854.

Aly M.H., Giardino J.R. and Klein A.G.; 2005: *Suitability assessment for New Minia City, Egypt: a GIS approach to engineering geology*. Environ. Eng. Geosci., 11, 259-269, doi: 10.2113/11.3.259.

Amano K., Toda T. and Abe H.; 1987: *Development and application of a hierarchical land-use model*. Mem. Fac. Eng., Kyoto Univ., 49, 326-357.

Arnous M.O.; 2013: *Geotechnical site investigations for possible urban extensions at Suez City, Egypt using GIS*. Arab. J. Geosci., 6, 1349-1369, doi: 10.1007/s12517-011-0441-1.

ASF Data Search; 2024: *ASF data search*. https://search.asf.alaska.edu/, accessed 15 December 2025.

Banai-Kashani R.; 1989: *A new method for site suitability analysis: the analytic hierarchy process*. Environ. Manage., 13, 685-693, doi: 10.1007/BF01868308.

Bastani M., Hashemi S., Khairabadi O. and Khavarian-Garmsir A.R.; 2024: *Assessing the resilience of informal urban settlements against earthquakes: a case study of Mashhad, Iran*. Nat. Hazards, 120, 4507-4526, doi: 10.1007/s11069-023-06381-4.

Collins M., Steiner F. and Rushman M.; 2001: *Land-use suitability analysis in the United States: historical development and promising technological achievements*. Environ. Manage., 28, 611-621, doi: 10.1007/s002670010247.

Dai F.C., Lee C.F. and Zhang X.H.; 2001: *GIS-based geo-environmental evaluation for urban land-use planning: a case study*. Eng. Geol., 61, 257-271, doi: 10.1016/S0013-7952(01)00028-X.

Darko A., Chan A.P.C., Ameyaw E.E., Owusu E.K., Pärn E. and Edwards D.J.; 2019: *Review of application of analytic hierarchy process (AHP) in construction*. Int. J. Constr. Manage., 19, 436-452, doi: 10.1080/15623599.2018.1452098.

Değerliyurt M.; 2014: *Settlement suitability analysis of local ground characteristics in Iskenderun: a case study*. Procedia - Soc. Behav. Sci., 120, 637-644, doi: 10.1016/j.sbspro.2014.02.144.

Erden T. and Karaman H.; 2012: *Analysis of earthquake parameters to generate hazard maps by integrating AHP and GIS for Küçükçekmece region*. Nat. Hazards Earth Syst. Sci., 12, 475-483, doi: 10.5194/nhess-12-475-2012.

Eren M.; 2026: *From linear model to machine learning algorithms: performance analysis of horizontal GNSS velocities of the coastal southern Scandinavia*. Bull. Geoph. Ocean., 67, 41-60, doi: 10.4430/bgo00507.

Fredlund D.G.; 2006: *Unsaturated soil mechanics in engineering practice*. J. Geotech. Geoenviron. Eng., 132, 286-321, doi: 10.1061/(ASCE)1090-0241(2006)132:3(286).

Hajilo M., Talkhab A. and Pennington-Gray L.; 2024: *Spatial analysis of earthquake-prone rural areas and residents' preparedness*. Nat. Hazards, 120, 4101-4130, doi: 10.1007/s11069-023-06364-5.

Harris B.; 1985: Urban simulation models in regional science. J. Reg. Sci., 25, 545-567.

Herbert J.D. and Stevens B.H.; 1960: *A model for the distribution of residential activity in urban areas*. J. Reg. Sci., 2, 21-36, doi: 10.1111/j.1467-9787.1960.tb00838.x.

Jara J.M., García-Calzada C., Olmos B.A. and Martínez G.; 2022: *Seismic response and reliability index of RC weak story buildings on soft soils of Mexico city*. J. Build. Eng., 50, 104199, doi: 10.1016/j.jobe.2022.104199.

Jha M.K., Chowdhury A., Chowdary V.M. and Peiffer S.; 2007: *Groundwater management and development by integrated remote sensing and geographic information systems: prospects and constraints*. Water Resour. Manage., 21, 427-467, doi: 10.1007/s11269-006-9024-4.

Kanlı A.I., Tildy P., Prónay Z., Pınar A. and Hermann L.; 2006: *Vs30 mapping and soil classification for seismic site effect evaluation in Dinar region, SW Turkey*. Geophys. J. Int., 165, 223-235, doi: 10.1111/j.1365-246X.2006.02882.x.

Karaoğlu G.T.; 2014: İstanbul *Küçükçekmece ilçesinin mühendislik jeolojisi ve yerleşime uygunluk değerlendirmesi*. Ph.D. Thesis, Institute of Science, Istanbul University, Istanbul, Turkey, 107 pp.

Köksalan M.M., Wallenius J. and Zionts S.; 2011: *Multiple criteria decision making: from early history to the 21st century*. World Scientific, Singapore, 212 pp., doi: 10.1142/8042.

Kramer S.L. and Stewart J.P.; 2024: *Geotechnical earthquake engineering, 2nd ed*. CRC Press, Boca Raton, FL, U.S.A., 1060 pp.

Liu R., Zhang L., Tang Y. and Jiang Y.; 2024: *Understanding and evaluating the resilience of rural human settlements with a social-ecological system framework: the case of Chongqing Municipality, China*. Land Use Policy, 136, 106966, doi: 10.1016/j.landusepol.2023.106966.

Malczewski J.; 2004: *GIS-based land-use suitability analysis: a critical overview*. Prog. Plann., 62, 3-65, doi: 10.1016/j.progress.2003.09.002.

Mitchell J.K., Soga K. and O'Sullivan C.; 2005: *Fundamentals of soil behavior, 3rd ed*. John Wiley & Sons, New York, U.S.A., 558 pp., doi: 10.1002/9781119832348.

Montoya L. and Masser I.; 2005: *Management of natural hazard risk in Cartago, Costa Rica*. Habitat Int., 29, 493-509, doi: 10.1016/j.habitatint.2004.04.003.

Orellana M.A., Ruiz S.E., Bojorquez J., Reyes-Salazar A. and Bojorquez E.; 2021: *Optimal load factors for earthquake-resistant design of buildings located at different types of soils*. J. Build. Eng., 34, 102026, doi: 10.1016/j.jobe.2020.102026.

Panahi M., Rezaie F. and Meshkani S.A.; 2014: *Seismic vulnerability assessment of school buildings in Tehran city based on AHP and GIS*. Nat. Hazards Earth Syst. Sci., 14, 969-979, doi: 10.5194/nhess-14-969-2014.

Putman S.H.; 1979: *Urban residential location models*. Springer, Dordrecht, The Netherlands, 169 pp., doi: 10.1007/978-94-009-9239-9.

Robertson P.K. and Wride C.E.; 1998: *Evaluating cyclic liquefaction potential using the cone penetration test*. Can. Geotech. J., 35, 442-459, doi: 10.1139/t98-017.

Romano G., Dal Sasso P., Liuzzi G.T. and Gentile F.; 2015: *Multi-criteria decision analysis for land suitability mapping in a rural area of Southern Italy*. Land Use Policy, 48, 131-143, doi: 10.1016/j.landusepol.2015.05.013.

Saaty R.W.; 1987: *The analytic hierarchy process - what it is and how it is used*. Math. Modell., 9, 161-176, doi: 10.1016/0270-0255(87)90473-8.

Santamarina J.C., Klein K.A. and Fam M.A.; 2001: *Soils and waves: particulate materials behavior, characterization and process monitoring*. John Wiley & Sons, Chichester, U.K., 512 pp.

Seed H.B. and Idriss I.M.; 1971: *Simplified procedure for evaluating soil liquefaction potential*. J. Soil Mech. Found. Div., 97, 1249-1273, doi: 10.1061/JSFEAQ.0001662.

Şener Ş., Şener E., Nas B. and Karagüzel R.; 2010: *Combining AHP with GIS for landfill site selection: a case study in the Lake Beyşehir catchment area (Konya, Turkey)*. Waste Manage., 30, 2037-2046, doi: 10.1016/j.wasman.2010.05.024.

Şeşetyan K., Demircioğlu Tümsa M.B. and Akinci A.; 2019: *Evaluation of the seismic hazard in the Marmara region (Turkey) based on updated databases*. Geosciences, 9, 489, doi: 10.3390/geosciences9120489.

Siddiqui M.Z., Everett J.W. and Vieux B.E.; 1996: *Landfill siting using geographic information systems: a demonstration*. J. Environ. Eng., 122, 515-523, doi: 10.1061/(ASCE)0733-9372(1996)122:6(515).

Tavana M., Soltanifar M. and Santos-Arteaga F.J.; 2023: *Analytical hierarchy process: revolution and evolution*. Ann. Oper. Res., 326, 879-907, doi: 10.1007/s10479-021-04432-2.

Tudes S. and Yigiter N.D.; 2010: *Preparation of land use planning model using GIS based on AHP: case study Adana-Turkey*. Bull. Eng. Geol. Environ., 69, 235-245, doi: 10.1007/s10064-009-0247-5.

Vaidya O.S. and Kumar S.; 2006: *Analytic hierarchy process: an overview of applications*. Eur. J. Oper. Res., 169, 1-29, doi: 10.1016/j.ejor.2004.04.028.

Wald D.J. and Allen T.I.; 2007: *Topographic slope as a proxy for seismic site conditions and amplification*. Bull. Seismol. Soc. Am., 97, 1379-1395, doi: 10.1785/0120060267.

Wang G., Qin L., Li G. and Chen L.; 2009: *Landfill site selection using spatial information technologies and AHP: a case study in Beijing, China*. J. Environ. Manage., 90, 2414-2421, doi: 10.1016/j.jenvman.2008.12.008.

Youssef A.M., Pradhan B. and Tarabees E.; 2011: *Integrated evaluation of urban development suitability based on remote sensing and GIS techniques: contribution from the analytic hierarchy process*. Arab. J. Geosci., 4, 463-473, doi: 10.1007/s12517-009-0118-1.

Corresponding author: Aziz Saraçoğlu
Department of Civil Engineering, Technology Faculty, Firat University,
Üniversite Street, Elazig, Turkey
Phone: +90 507 159 2607; e-mail: asaracoglu@firat.edu.tr